ICAS 2021 SHANGHAI International Council of the Aeronautical Sciences
32nd Congress of the International Council of the Aeronautical Sciences
September 6-10, 2021 Pudong Shangri-La, Shanghai, China

EXPERIMENTAL RESEARCH ON PROPULSION AND AERODYNAMIC CHARACTERISTICS OF A DUAL-BODY DISTRIBUTED ELECTRIC PROPULSION AIRCRAFT

Zhang Xingyu[1,2], Gao Zhenghong[1,2], Lei Tao[1,3], Zhang Xiaobin[1,3]& Zhang Wei[1,2]

[1]Key Laboratory of Aircraft Electrical Propulsion Technology (Ministry of Industry and Information Technology), Northwestern Polytechnical University, 710072, Xi'an P.R.China

[2] School of Aeronautics, Northwestern Polytechnical University, 710072, Xi'an P.R.China

[3] School of Automation, Northwestern Polytechnical University, 710072, Xi'an P.R.China

Abstract

Distributed Electric Propulsion (DEP) aircraft shows great potential for Green Aviation application because of its high energy efficiency propulsion system. However, compared with the traditional aircraft configuration which using fossil fuel like kerosene and gasoline, the DEP aircraft has shown a strong aerodynamic propulsion coupling phenomenon. In order to explore the aerodynamic propulsion coupling characteristics of DEP aircraft, a set of low-cost DEP aircraft aerodynamic/propulsion system ground-based testbed is designed, Then, the aerodynamic/thrust coupling characteristics of a DEP Technology Verification UAV are studied by ground experiment. The results show that the Electric Ducted Fan (EDF) provided the suction effect on the boundary layer which accelerates the air flow on the upper wing, leads to a larger pressure difference between the upper and lower wings then increases the Lift. And the phenomenon of the aerodynamic center moves backward should be paid attention to, it may attribute to the nonlinear increased Lift. The research results provide a reference for the overall design of DEP aircraft.

Keywords: Distributed Electric Propulsion; Ground Experiment; Aerodynamic Propulsion Coupling; Electric Ducted Fan; Boundary Layer Suction

1. Introduction

Since the environment protection plays significant role in universal transportation, and its importance is increasing day by day, we now facing the challenge to use up-dated technology and new concepts to meet the need of Green Aviation. NASA's New Generation (N+3) subsonic aircraft performance target and EU's "flightpath 2050" Plan set requirements for future aircraft fuel consumption, exhaust emission and noise level which were much higher than today's standard [1]. Due to the fuel efficiency limitation of the fossil fuel powered power unit, it is difficult to make a breakthrough in propulsion efficiency and emission. While electric as a widely used secondary energy, with low noise and almost no impact to the environment [2], has become the main energy form in the research of Green Aviation.

The electric aircraft propulsion system using electric as the main energy source, and the scale-invariant characteristic of the electric motor system has potential advantages. The distributed electric propulsion configuration is much more flexible to meet the design requirements. And combined with the technics such as the Boundary Layer Ingestion (BLI), the aerodynamic and propulsion efficiency can be improved and eventually archive the optimal integration of aerodynamics, structure, and power [3]. But at the same time, the distributed thrusters installed on the trailing edge of wing produced the strong coupling phenomenon between the aerodynamic characteristics and propulsion characteristics of the DEP aircraft. Furthermore, the suction effect of the propulsion unit on the boundary layer can reduce the Drag. Therefore, distributed propulsion unit can increase Lift and reduce Drag, and improve aircraft aerodynamic efficiency [21]. For the ordinary configuration aircraft, the flow through the aircraft will reduce the flow velocity and form a low-speed wake area at the rear of the aircraft, which will reduce the propulsion efficiency of the aircraft. However, the distributed powered aircraft can partially or even completely fill the low-speed wake area through the propulsion unit installed at the trailing edge of the wing, which can improve the propulsion efficiency and save fuel [4].

Due to these advantages mentioned above, the research of the DEP aircraft became the universal trend. The most famous cases are NASA's X-57 Maxwell test aircraft [5] and German Lilium aviation's Lilium jet [7]. Researchers have done a lot of research on the key technologies of DEP aircraft. Wang et al. [8] studied the design method of distributed hybrid UAV power system. Kerho et al. [9,10] used Computational Fluid Dynamics (CFD) and wind tunnel experiments to study the influence of thrusters on wing aerodynamic performance of a small DEP vehicle. Pieper et al. [11] developed a dynamic scaling Verification UAV for DEP aircraft with the support of NASA STTR project and determined the propeller layout by using the thrust line method.

Other research shows that there is a strong coupling effect between aerodynamics and propulsion of DEP aircraft [12,13]. The traditional aerodynamic analysis method based on engineering experience cannot meet the design requirement of DEP aircraft [12]. Recent researcher was focused on the layout design, the power system evaluation, and the coupling effect between the power and aerodynamic of the DEP aircraft [14-18]. The ground-based vehicle experiment can save a lot of time and cost than the wind tunnel test, at the same time, and it is easier to evaluate the aerodynamic performance of the aircraft, thus saving the development time [19].For example, NASA has constructed the HEIST testbed (Hybrid Electric Integrated Systems Testbed) to investigate the Aerodynamic/Propulsion coupling characteristics and power system characteristics of the X-57 Maxwell DEP aircraft, as shown in Figure 1 [20]. The research results show that: by using the DEP technology, the maximum Lift Coefficient of the aircraft in the take-off and landing configuration is improved, only 42% of the original wing area is needed to fulfill the cruising Lift requirement. Besides, it can reduce the Drag in cruise configuration, but it will bring a large nose down Pitch Moment.

Figure 1 – The NASA HEIST Testbed.

Because the DEP Verification UAV designed by our laboratory used a different aircraft configuration to the NASA's X-57 Maxwell Aircraft, the aerodynamic/propulsion coupling characteristics are also different.

This paper is mainly focused on following contents: To explore the power system and aerodynamic/propulsion coupling characteristics of our DEP Verification UAV, especially to conduct the quantitative analysis of the Lift and Pitching Moment of the Distributed Ducted Electric Fan Propulsion system installed on wing's trailing edge. And to speed up the iteration process of the DEP Verification UAV design. A ground testbed for the aerodynamic / propulsion system of DEP aircraft is established, and the Thrust/Lift coupling characteristics of the power system of DEP aircraft are studied by ground-based experiment.

2. Overall Design Parameters and Characteristics of the Distributed Electric Propulsion Technology Verification UAV

The distributed electric propulsion technology Verification UAV designed by the laboratory is an exploration and demonstration testbed for DEP technology, which is mainly used to explore and verify DEP technology, including Aerodynamic/Propulsion coupling effect, thrust control technology, energy optimization and management technology, flight safety and reliability and other key technologies.

Considering the manufacturing cost and equipment configuration, the Verification UAV uses the dual fuselage with tandem wing configuration. The fuselage is 2400mm long, the wingspan of front wing is 2680mm and 4314mm for the main wing, using NACA4415 airfoil. The front wing area is 0.804m^2, and the rear wing area is 1.368m^2. Theoretically, the dual fuselage tandem wing configuration can make the Verification UAV obtain better aerodynamic performance. The downwash of the front wing can reduce the effective angle of attack of the rear wing. Therefore, when the front wing stalls, the rear wing can stay in the safety zone of angle of attack (AOA), which can delay the stall and improve the maximum Lift Coefficient of the whole aircraft. The change of Lift force on the front and rear wings will produce a nose-down moment, which can make the aircraft recovery from stall.

The Power Unit configuration of the DEP Verification UAV is different from NASA's X-57 DEP aircraft. For NASA's X-57, the power unit is installed at the leading edge of the wing to improve the aerodynamic efficiency through the slipstream effect of the propeller. But for our Verification UAV, the power unit is installed at the wing's trailing edge to utilize the BLI effect which can increase the Lift and reduce the Drag. And by deflecting the trailing edge, the vector thrust can be used as an attitude control surface and able to archive short takeoff and landing (STOL) at the same time,

The whole aircraft is equipped with 24 electric ducted fans (EDF) divided into four sets of power units, each one includes six EDFs. The power sets is respectively arranged at the front wing's trailing edge of the middle wing section and the rear wing's trailing edge of the left/middle/right wing section. In total, the aircraft is equipped with The aircraft configuration is shown as in Figure 2.

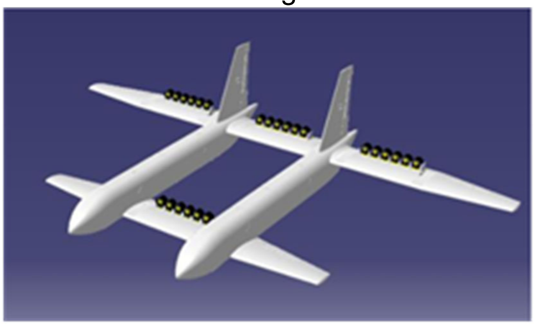

Figure 2 – Configuration of DEP Technology Verification UAV

During the conceptual design, the aerodynamic characteristics of the Verification UAV were briefly assessed by numerical method and the characteristics can be summarize as follows:

(1) The aircraft can achieve the maximum Lift Drag ratio 9 and Lift Coefficient is 0.62 at 3.5°AOA,with no longitudinal pitching moment. It is not necessary to deflect the elevator to trim the aircraft at this AOA, which can reduce the trim Drag force. Therefore, 3.5° AOA is selected as the cruise angle of attack of this aircraft in the experiment.

(2) Because the power system using EDFs installed above the wing, and the thrust does not through UAV's center of gravity, and the thruster installed on the front wing is less than rear wing, the propulsion system will produce a variable nose-down moment to the whole aircraft during flight, and the elevator needs to be deflected to trim the UAV.

(3) Because of the dual fuselage configuration, the wetted area of the aircraft is increased, which brings additional friction, so the Lift to Drag ratio of the whole aircraft is reduced. The Lift/Drag ratio is only 9 and is much lower than recent designed aircraft, but we mainly focused the change of the Lift to quantify the Aerodynamic effect of the Power unit.

(4) When the Center of Gravity of the UAV is between the front and rear wings and 0.868m away from the leading edge of the front wing, the static stability margin is 15.38%. Generally, to archive

good static stability and maneuverability, the static stability margin of small and medium UAVs is between 10% to 20%.

In general, the DEP technology Verification UAV's aerodynamic performance and stall characteristics are both excellent, and the Pitching Moment Coefficient of the whole UAV is close to zero at the maximum Lift to Drag ratio state, so the additional trim drag is relatively small. Meanwhile, the position of the center of gravity and the moment reference point in the follow-up experiment are determined.

3. Ground-Based Distributed Electric Propulsion Aircraft System Testbed

Because the complex coupling mechanism between EDFs and wing, and the performance test for the on-shelf EDF power unit is needed. A ground-based DEP aircraft system testbed was established to evaluate the performance of EDF and aerodynamic/propulsion coupling characteristics.

3.1 Electric Ducted Fan Propulsion System Testbed

To shorten the development period and reduce the cost, instead of design a new EDF for the DEP Verification UAV propulsion system, we decided to select a suitable shelf product according to the performance requirements of the UAV. But at present, the choice of EDF for UAV is limited, there are very few professional EDF products on the market, and most of the shelf products are low-cost products for entertainment aviation model. Due to the cost limitation, the workmanship is generally rough, performance consistency is poor, and usually cannot achieve the performance they claimed.

Therefore, to evaluate and obtain the accurate performance of EDF, a propulsion system performance testbed is designed, as shown in Figure 3. The testbed is composed of thrust measurement system, electric power supply system and data measurement system and can support up to six EDFs.

Figure 3 – Ground Based Testbed for the Electric Ducted Fan Propulsion System

As an important device, the power supply system providing electric energy for EDF motor. According to the rated voltage and power demand of EDF, a 15KVA (DC30V / 500A) programmable high-power regulated DC power supply is used, which can supply electric energy for six EDFs with rated voltage below 30V and rated power below 1.5kw. A 15VDC switching power supply is used to supplies power for the load cells, current sensors, and signal conditioning board.

The EDF was installed on the structure frame of the thrust measurement system, the thrust and gross weight can be measured by the load cells. The change of the mass of the installation assembly under different thrust conditions can be regarded as the measurement value of thrust.

The parameter measurement system of electrical power mainly measures the current of the EDF under the voltage variation range of lithium battery (16.8-14.8VDC) under different thrust. We use LEM It-508 / S6 current sensor for main bus current measurement, and the LT-108 / S7 for brunch current measurement. The mass signal of EDF installation assembly measured by the load cell, the current signal output by current sensors and the voltage signal collected from main bus are connected to the signal conditioning board. After signal conditioning, the real-time signal acquisition system based on Ni PXI with single channel sampling frequency of 250kS/s is used for data acquisition under LabVIEW software environment.

3.2 Vehicle Based Testbed For Aerodynamic Characteristics Of Distributed Electric Propulsion Verification UAV

Before the UAV’s first flight, the Aerodynamic characteristics including Lift, Pitch Moment and Aerodynamic Center of the aircraft should be evaluated to ensure the first flight safety. The vehicle-based experiment is a relatively simple engineering experiment method to measure the Lift, Pitch Moment and other forces and moments of the DEP technology Verification UAV.

The DEP Technology Aircraft Vehicle-Based Testbed is equipped with an experiment structure including a measurement system on the top of the experiment vehicle, as shown in Figure 4.

Figure 4 – Ground Vehicle-Based Testbed of the DEP Verification UAV

The landing gear of the verification UAV was used as the fixing joints and fixed to the testbed frame through the connecting mechanism, which connected to the load cells. The testbed structure was built by aluminum profile and stainless steel, and the measurement system is composed of several load cells, transmitters, current sensors, signal acquisition cards and data processing software. The force signal was measured by L6N-C3-30Kg load cell manufactured by ZEMIC, then converted into voltage signal by FD-3 signal transmitter also manufactured by ZMEIC. The analog signal was acquired by the signal conditioning board and NI-PXI real-time signal acquisition system under LabVIEW software environment. Before the experiment, all force sensor is calibrated by standard weights. After calibration, the system measurement error is less than 2% F.S.

The testbed installed on the vehicle can simulate the flying state by driving the vehicle at a constant speed. The weight change of the UAV can be measured by the load cells. The Lift can be obtained by UAV’s weight change. The Pitch Moment can be calculated by the distance between front and rear wheel and the force changes. The concept of measurement is as follows:

$$\mathrm{W}_{GrossWeight} = \mathrm{W}_{LeftFront} + \mathrm{W}_{RightFront} + \mathrm{W}_{LeftBack} + \mathrm{W}_{RightBack} \tag{1}$$

$$\mathrm{W}_{Front} = \mathrm{W}_{FL} + \mathrm{W}_{FR} \tag{2}$$

$$\mathrm{W}_{Left} = \mathrm{W}_{FL} + \mathrm{W}_{RL} \tag{3}$$

$$\mathrm{X}_{COG} = \frac{\mathrm{W}_{Front,\ \alpha=0}}{\mathrm{W}_{GrossWeight}} \times \mathrm{L}_{Wheel-Base} \tag{4}$$

$$Y_{COG} = \frac{\mathrm{W}_{Left,\ \alpha=0}}{\mathrm{W}_{GrossWeight}} \times \mathrm{L}_{Wheelspan} \tag{5}$$

$$\mathrm{L}_{Lift} = \Delta\mathrm{W}_{LeftFront} + \Delta\mathrm{W}_{RightFront} + \Delta\mathrm{W}_{LeftBack} + \Delta\mathrm{W}_{RightBack} \tag{6}$$

$$\mathrm{M}_{y} = \mathrm{X}_{COG} \times \Delta\mathrm{W}_{Front} - \left(\mathrm{L}_{Wheel-Base} - \mathrm{X}_{COG}\right) \times \Delta\mathrm{W}_{Back} \tag{7}$$

$$\mathrm{M}_{\mathrm{x}} = Y_{COG} \times \Delta\mathrm{W}_{Left} - \left(\mathrm{L}_{Wheelspan} - \mathrm{Y}_{COG}\right) \times \Delta\mathrm{W}_{Right} \tag{8}$$

However, the Drag of UAV cannot be measured by the sensor installed in the vertical direction. If the Drag data needs to be measured, a six-component balance should be added. Limited by the experimental conditions, only the Lift and Pitch Moment data were measured and analyzed in this experiment.

It is worth noting that the aerodynamic interference between the experiment vehicle and the aircraft should be considered when using this experiment method to evaluate aerodynamic force, such as how to eliminate the influence of upwash caused by the front windshield of the vehicle, and how to limit the deformation of the fuselage which could add internal stress to the force measuring mechanism and influence the results.

Figure 5 – Ground Vehicle-Based Testbed with Flow Divider

Since the cost to build a truck based testbed like NASA's HEIST Testbed is unaccepted for us and the car we used can only bear stuff under 100KG on the roof rack. The distance of install surface to the roof was limited to 500mm. To solve these problems properly, a flow divider was installed at the front of the vehicle, as shown in Figure 5, through testing and calibration, the influence of upwash flow can be reduced to about 3°. At the same time, to improve the rigidity of the fuselage, a rigid rod is added at the connect joint to strengthen the testbed frame and the aircraft, which improves the rigidity of the aircraft and eliminates the internal stress.

4. Results Analysis of Ground Experiment

4.1 Experiment Results of Electric Ducted Fan Propulsion System

Firstly, the electric ducted fan performance experiment is carried out to verify and compare the performance of different off-shelf EDFs selected for the power system.

Table 1 EDF Product Parameters Index

	EDF-A QX-12	EDF-B QX-6	EDF-C FMS
Claimed Thrust / g	1800	2050	1630
Rated Voltage / V	14.8	14.8	16.5
Rated Current / A	62	74	64
Rated Power / W	918	1095	1056
Mass / g	173	167	165
KV Value	2600	3800	2750

The thrust experiment of three EDFs was carried out, and the voltage, current, rev, thrust and other parameters under different working conditions were measured, and the thrust characteristics were compared in detail.

As can be seen from figure 6-8, QX-6's maximum thrust and efficiency does not meet the selection requirements. The FMS EDF has similar performance with QX-12 in all specs, but its efficiency is lower than QX-12 in high revs, and its maximum thrust is also smaller, so the final selection result is QX-12 EDF.

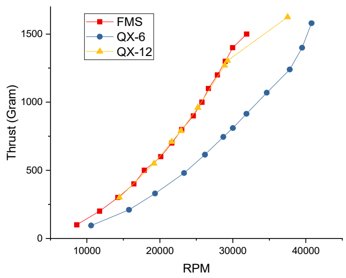

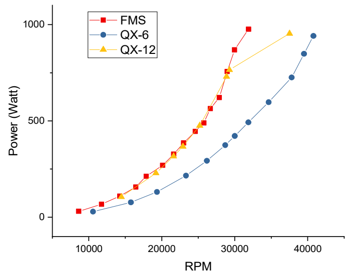

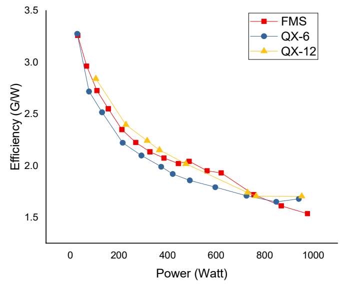

Figure 6 – Thrust Curve of EDF Figure 7 – Power Curve of EDF Figure 8 – Efficiency Curve of EDF

After the EDF performance test, to evaluate the full voltage range operation characteristics of the selected EDF, the output voltage of the Li-Po battery will change from 16.8v to 14.8V according to its SOC (state of charge). The power system ground testbed is used to accomplish the evaluation experiment, and the results are shown in Figure 9-10 below:

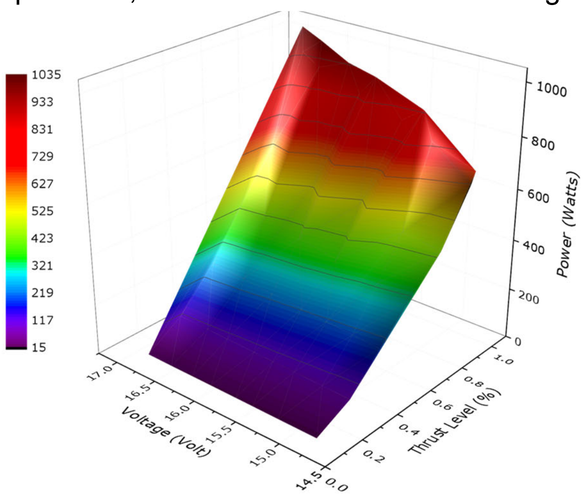

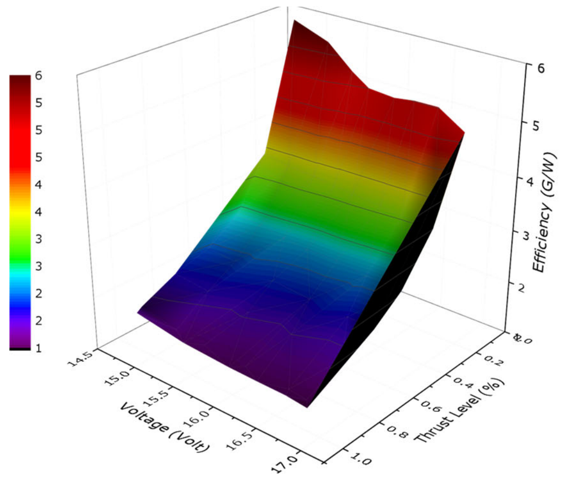

Figure 9 Thrust under Li-Po Battery Voltage Figure 10 Efficiency under Li-Po Battery Voltage

Under battery operating voltage range (14.5-16.8v), the change of power and thrust to voltage is basically linear for QX-12 EDF, and the gradient of thrust increases with the increase of operating voltage, but the efficiency decreases. Under the stable cooling condition, the maximum thrust is 1150g-1475g (14.8v-16.8v), the maximum power is 668w-1035w (14.8v-16.8v), and the force efficiency is 1.71-1.42g/w (14.8v-16.8v).The theoretical maximum thrust in the horizontal direction can reach 35.4kg when the aircraft lithium battery is fully charged, and 27.6kg when the lithium battery is almost dead. Although there is a difference between the actual and claimed performance, it still meets the power demand of the conceptual design.

4.2 Experiment Results of Distributed Electric Propulsion Aircraft Aerodynamic/Propulsion Coupling Characteristics

After power system experiment, according to the results, the selected EDFs were installed on the Verification UAV, and a vehicle-based testbed for the aerodynamic characteristics of DEP aircraft is built to carry out a preliminary exploration on the aerodynamic/propulsion coupling characteristics. The aerodynamic characteristics of the aircraft are evaluated through the experiment under different speed (15/20/25m/s), thrust (t=0/15/20/25/30/35/45%) and AOA(5°/9°/11°/17°/18°).

During the experiment, the driver drove the experiment vehicle to reach the required airspeed for the UAV in a straight runway, acquired the reading from testbed. Although there were errors and fluctuations in the data obtained from the vehicle-based testbed, it is basically stable within a certain range. The UAV aerodynamic data can be obtained through Moving Average Filtering.

Due to the influence of the vehicle to the flow field, a baseline test is performed, and comparing the measured value of the angle of attack sensor with the geometric angle between the test structure and the fuselage, it can be found that the fuselage causes 10°-12° upwash and affected the accuracy of the experimental results. To minimize the influence of upwash airflow, a Flow Divider is set up in the front of the vehicle, and the gaps and holes between the aircraft and the roof were covered, the influence of the vehicle on the AOA could reduce to 3°. The AOA sensor reading is used to represent the actual angle of attack instead of the geometric angle between the aircraft and the test frame, then conducted the experiment to measure the Lift and Pitching Moment at different actual AOA.

Figures 11 to 16 show the curves of Lift and moment VS thrust at different airspeed after applied the Moving Average Filtering and using actual AOA.

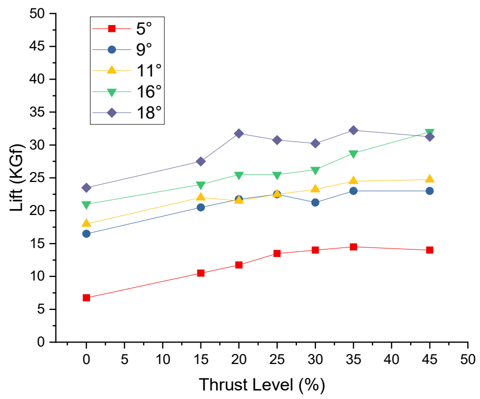

Figure 11 Lift vs Thrust Level at 15m/s

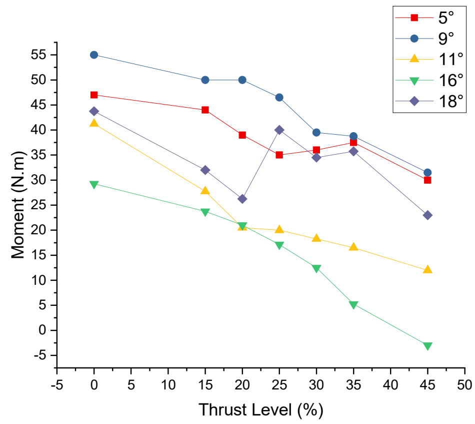

Figure 14 Pitch Moment vs Thrust Level at 15m/s

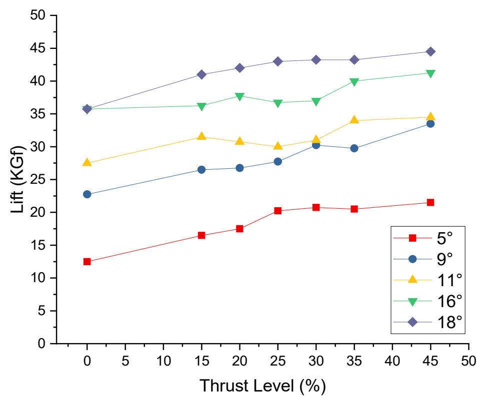

Figure 12 Lift vs Thrust Level at 20m/s

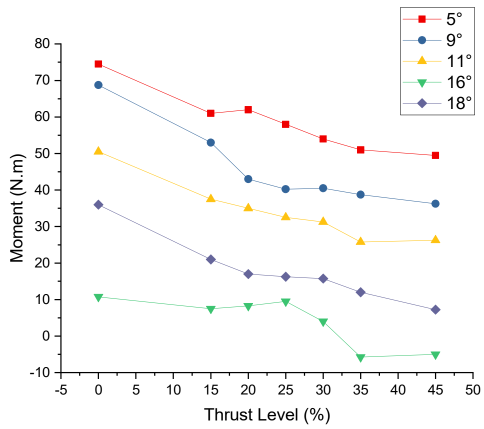

Figure 15 Pitch Moment vs Thrust Level at 20m/s

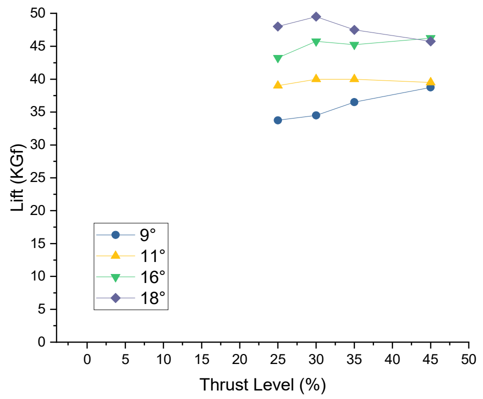

Figure 13 Lift vs Thrust Level at 25m/s

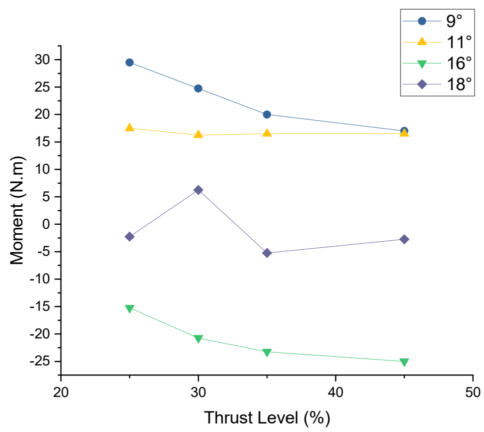

Figure 16 Pitch Moment vs Thrust Level at 25m/s

By analyzing the experimental data, the following phenomena can be concluded

1) There is a strong coupling between the aerodynamic characteristics of the whole aircraft and the propulsion device, and it is related to the airspeed. As the propulsion power increases, so does the Lift. Taking throttle signal (represented by throttle signal PWM Duty Ratio) as variable:

   At the airspeed of 15 m/s with power, compared with no propulsion state, the maximum Lift at low AOA can be increased by 114%: at medium AOA by 40%, and at high AOA by 32-38% with propulsion.

   At the airspeed of 20 m/s with power, compared with no propulsion state, the maximum Lift at low AOA can be increased by 72%, at medium AOA by 40%, and at high AOA by 15-25% with propulsion.

   At the airspeed of 25 m/s with power, compared with 25% thrust level, the maximum Lift at low AOA can be increased by 15% with 45% thrust level. However, in the high AOA, the increase is not obvious, and its mechanism needs to be further studied.

   In general, the DEP power system can improve the Lift of the wing, especially in the case of low speed and small AOA, its Lift increasing effect is more obvious, and its suction to the boundary layer of the wing can effectively reduce the airflow separation, which is conducive to the stall characteristics and can reduce Drag.

2) As the propulsion device has a great influence on the Lift, it can be seen from figure 14-16 that with the increase of thrust, the aircraft pitching moment (nose-up as positive) decreases at various airspeeds and AOA, that is, increases the nose-down pitching moment. At the same time, after processing the experimental data, compared with the theoretical calculated aerodynamic center position which is 818 mm away from the leading edge of the front wing at the cruise AOA, the actual aerodynamic center position moves back to 1169.14 mm at the speed of 20 m/s, and to 1441.98 mm at 25 m/s.

   The reason of pitching moment increases, and Aerodynamic Center backward shift of propulsion device is that the nonlinear Lift increment induced by propulsion device is obvious, and the proportion of rear power unit and rear wing area is relatively large. When the thrust is changed, the Lift increment of rear wing is obvious, and the aerodynamic center moves backward, which ultimately affects the stability of aircraft. This phenomenon is different from that of conventional layout aircraft. Therefore, in the design of DEP aircraft, it is necessary to pay special attention to the influence of nonlinear Lift increment on aircraft stability and the influence of distributed power unit configuration on aerodynamic characteristics. In addition, the nonlinear Lift increment caused by distributed power system puts higher requirements for the design of flight control system. Further research on its internal mechanism is needed in the follow-up research.

Copyright Statement

References

[1] KONG Xianghao, ZHANG Zhuoran, LU Jiawei, LI Jincai, YU Li. Review of electric power sys-tem of distributed electric propulsion aircraft[J]. ACTA AERONAUTICAET ASTRONAUTICA SINICA, 2018, 39(1): 21651-021651.

[2] HUANG Jun, YANG Feng-tian. Development and challenges of electric aircraft with new energies[J]. ACTA AERONAUTICAET ASTRONAUTICA SINICA, 2016, 37(1): 57-68.

[3] Wang Mi-aoxiang，Wang Yuanyuan. Review on misconceptions of electric propulsion aircraft analysis and re-search[J]. Aeronautical Science & Technology，2019，30（05）：3-8.

[4] STEINER H J, SEITZ A, WIECZOREK K, et al. Multidisciplinary design and feasibility study of distributed propulsion systems[C]//28th International Congress of the Aeronautical Sciences. 2012: 23-28.

[5] KO A, SCHETZ J A, MASON W H. Assessment of the potential advantages of distributed propulsion for aircraft[C]//XVIth International Symposium on Air Breathing Engines (ISABE), Cleveland, OH, Paper. 2003, 1094.

[6] HOOVER C B, SHEN J, KRESHOCK A R. Propeller Whirl Flutter Stability and Its Influence on X-57 Air-craft Design[J]. Journal of Aircraft, 2018, 55(5): 2169-2175.

[7] KIM H D, PERRY A T, ANSELL P J. A review of distributed electric propulsion concepts for air vehicle technology[C]//2018 AIAA/IEEE Electric Aircraft Technologies Symposium (EATS). IEEE, 2018: 1-21.

[8] WANG S, ECONOMOU J T, TSOURDOS A. Indirect engine sizing via distributed hybrid-electric unmanned aerial vehicle state-of-charge-based parametrization criteria[J]. Proceedings of the Institution of Mechanical Engineers, Part G: Journal of Aerospace Engineering, 2019, 233(14): 5360-5368.

[9] KERHO M F. Aero-propulsive coupling of an embedded, distributed propulsion system[C]//33rd AIAA Applied Aerodynamics Conference. 2015: 3162.

[10]KERHO M, KRAMER B. Turboelectric distributed pro-pulsion test bed aircraft[J]. Rolling Hills Research Corporation, El Segundo, Tech. Rep, 2013.

[11]PIEPER K, PERRY A, ANSELL P, et al. Design and Development of a Dynamically, Scaled Distributed Electric Propulsion Aircraft Testbed[C]//2018 AIAA/IEEE Electric Aircraft Technologies Symposium (EATS). IEEE, 2018: 1-2.

[12][BORER N K, DERLAGA J M, DEERE K A, et al. Comparison of aero-propulsive performance predictions for distributed propulsion configurations [C]//55th AIAA Aerospace Sciences Meeting. 2017: 0209.

[13]SCHETZ J A, HOSDER S, DIPPOLD III V, et al. Pro-pulsion and aerodynamic performance evaluation of jet-wing distributed propulsion[J]. Aerospace Science and Technology, 2010, 14(1): 1-10.

[14]LEIFSSON L, KO A, MASON W H, et al. Multidisciplinary design optimization of blended-wing-body transport aircraft with distributed propulsion[J]. Aerospace Science and Technology, 2013, 25(1): 16-28.

[15]MA Y, ZHANG W, ZHANG Y, et al. Effects of Distributed Propulsion Crucial Variables on Aerodynamic and Propulsive Performance of Small UAV[C]//Asia-Pacific International Symposium on Aerospace Technology. Springer, Singapore, 2018: 1535-1550.

[16]YOO S, DUENSING J. Computational Analysis of the External Aerodynamics of the Unpowered X-57 Mod-III Aircraft[C]//AIAA Aviation 2019 Forum. 2019: 3698.

[17]DEERE K A, VIKEN S, CARTER M, et al. Computation-al analysis of powered lift augmentation for the LEAPTech distributed electric propulsion wing [C] //35th AIAA Applied Aerodynamics Conference. 2017: 3921.

[18]DEERE K A, VIKEN J K, VIKEN S, et al. Computational analysis of a wing designed for the X-57 distributed electric propulsion aircraft[C]//35th AIAA applied aerodynamics conference. 2017: 3923.

[19]JIA Yi, ZHANG Yongsheng, LIU Dan, et al. A ground test vehicle (GTV) system to measure the aerodynamic characteristics of unmanned air vehicles[J]. Journal of Experiments in Fluid Mechanics (in Chinese), 2013, 27(3):81-86.

[20]DUBOIS A, VAN DER GEEST M, BEVIRT J B, et al. Design of an Electric Propulsion System for SCEPTOR[J]. 2016.

[21]STOLL A M, BEVIRT J B, MOORE M D, et al. Drag reduction through distributed electric propulsion[C]//14th AIAA aviation technology, integration, and operations conference. 2014: 2851.